Hydration sphere structure of architectural molecules: polyethylene glycol and polyoxymethylene oligomers

Ahmed M. Rozza[1,2], Danny E. P. Vanpoucke[3,*], Eva-Maria Krammer[4], Julie Bouckaert[4], Ralf Blossey[4], Marc F. Lensink[4], Mary Jo Ondrechen[5], Imre Bakó[6,*], Julianna Oláh[1,*], Goedele Roos[4,*]

[1] Department of Inorganic and Analytical Chemistry, Budapest University of Technology and Economic, Budapest, Hungary
[2] Department of Biotechnology, Faculty of Agriculture, Al-Azhar University, Cairo 11651, Egypt
[3] UHasselt, Institute for Materials Research, Diepenbeek, Belgium, IMOMEC, IMEC vzw, Diepenbeek, Belgium, Department of Electromechanical, Systems and Metal Engineering, Ghent University, Belgium
[4] Univ. Lille, CNRS, UMR 8576 - UGSF - Unité de Glycobiologie Structurale et Fonctionnelle, F-59000 Lille, France
[5] Department of Chemistry and Chemical Biology and Department of Bioengineering, Northeastern University, Boston, MA 02115 USA
[6] Institute of Organic Chemistry, Research Centre for Natural Sciences, Hungarian Academy of Sciences, Budapest, P.O. Box 286, Hungary

[*] Goedele Roos : Univ. Lille, CNRS, UMR, UGSF- Unité de Glycobiologie Structurale et Fonctionnelle, 8576, 50 avenue de Halley 59658 Villeneuve d'Ascq, F-59000 Lille, France, goedele.roos@univ-lille.fr
Danny E. P. Vanpoucke : UHasselt, Institute for Materials Research, Agoralaan, Building D, room D-F2.04, 3590 Diepenbeek, Belgium, danny.vanpoucke@uhasselt.be
Imre Bakó : Institute of Organic Chemistry, Research Centre for Natural Sciences, Hungarian Academy of Sciences, Magyar tudósok körútja 2, H-1519 Budapest, P.O. Box 286, Hungary, bako.imre@ttk.hu
Julianna Oláh : Department of Inorganic and Analytical Chemistry, Budapest University of Technology and Economic, Műegyetem rkp. 3., H-1111 Budapest, Hungary, olah.julianna@vbk.bme.hu

ORCID ID :
Ahmed M. Rozza : 0000-0002-2444-5069
Danny E. P. Vanpoucke: 0000-0001-5919-7336
Julie Bouckaert : 0000-0001-8112-1442
Ralf Blossey: 0000-0002-4823-7037
Marc F. Lensink : 0000-0003-3957-9470
Mary Jo Ondrechen : 0000-0003-2456-4313
Julianna Oláh: 0000-0003-4608-3115
Goedele Roos : 0000-0003-1450-2485

Keywords : solvation, atomic charge, hydrogen bond, topological analysis, molecular dynamics simulation, quantum chemical calculation

TOC-graphics

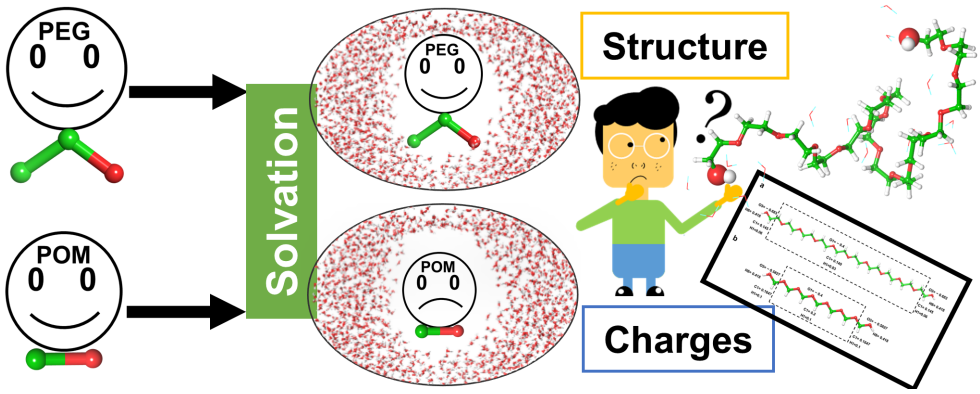

Abstract

Non-toxic, chemically inert, organic polymers as polyethylene glycol (PEG) and polyoxymethylene (POM) have versatile applications in basic research, industry and pharmacy. In this work, we aim to characterize the hydration structure of PEG and POM oligomers by exploring how the solute disturbs the water structure compared to the bulk solvent and how the solute chain interacts with the solvent. We explore the effect of (i) the C-C-O (PEG) versus C-O (POM) constitution of the chain and (ii) chain length. To this end, MD simulations followed by clustering and topological analysis of the hydration network, as well as by quantum mechanical calculations of atomic charges are used.

We show that the hydration varies with chain conformation and length. The degree of folding of the chain impacts its degree of solvation, which is measurable by different parameters as for example the number of water molecules in the first solvation shell and the solvent accessible surface. Atomic charges calculated on the oligomers in gas phase are stable throughout conformation and chain length and seem not to determine solvation. Hydration however induces charge transfer from the solute molecule to the solvent, which depends on the degree of hydration.

1. Introduction

Long-chained organic polymers, which are composed of numerous repeating monomer units, are frequently used in a variety of industrial, agricultural, and medical applications[1–4]. For example, polyethylene glycol (PEG) − a polymer made up of various units of ethylene glycol $(CH_2CH_2O)_n$ − is nontoxic, chemically inert, non-antigenic, highly soluble in water and in ethanol and has a high biocompatibility[5,6]. Along with these characteristics, PEG is FDA approved as an architectural molecule in for example drug carriers or multivalent inhibitors[7].
They can reduce the immunogenicity of biosimilar therapeutics and decrease renal clearance.
PEG also serves as a model system to investigate the intricate behavior of polymers in solution[8,9]. Hydration of these polymers modulates the chain's characteristics. The perturbation caused by the hydrogen bond formation in the coordinated water networks will determine the physical properties and has a profound effect on, *e.g.*, chemical reactions in the solvent and on the ability to bind as a ligand in, *e.g.*, protein cavities.

In the present study, due to their versatile applications in both basic research and industry, we direct our attention to PEG and polyoxymethylene (POM) which differ in the constitution of the polymer backbone: PEG is characterized by repeating units of C-C-O, while in POM C-O units are repeated (see Chart 1).

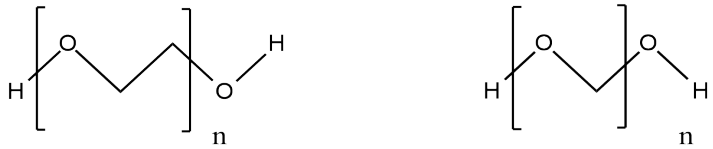

n= 2, 3, 5, 10, 15, 25, 50 — Models of PEG

n= 3, 7, 13, 22 — Models of POM

Chart 1. Building blocks of PEG and POM oligomers showing also the number of units (n) that build up the chains studied in this work.

Oligomers of different lengths as models for PEG and POM polymers are chosen to explore the effects of (i) the C-C-O (PEG) versus C-O (POM) constitution of the chain and (ii) chain length. We investigate how the solute disturbs the water structure compared to the bulk solvent and how the solute chain interacts with the solvent.

While PEG is soluble in water[10], POM is completely insoluble and even in apolar solvents such as benzene and toluene, high temperatures are needed to dissolve it. The contrast between the solubilities of PEG and POM in water is counterintuitive based on their C/O ratios. A recent publication by Ensing *et al.* [11] sought to explain the solubility patterns in water using MD simulations on PEG-3 and POM-3 chains. They discuss inductive effects of the intrinsically different polarization of the single bonds of the backbone chain (formally C has an oxidation number of 0 in POM and -1 in PEG.), resulting in different partial RESP charges (Restrained Electro-Static Potential charges, characteristic charges for describing the electrostatic interaction at large distance from the molecule) on the ether oxygen atoms in POM and PEG, as the underlying factor determining solvation. Using different atomic charge schemes and longer PEG/POM chains, we refine this finding. We show that solvation varies with chain conformation and chain length, while the atomic charge calculated on the oligomers in gas phase does not. The degree of folding of the chain impacts its degree of solvation, which is measurable by different parameters as for example the number of water molecules in the first solvation shell and the solvent accessible surface. For less solvated chains, a lower charge transfer from the solute to the solvent is found.

The structure of solvation networks can be characterized using the toolbox of complex network theory[12]. Also biopolymer solvation is well studied[13,14]. PEG in water is stabilized by water bridges[15,16]. Earlier studies report that hydrated PEG polymers form helical structures for which the surface hydrophobicity increases with chain length[17]. Hydration stiffens the PEG polymer by stabilizing the local helical structure elements through the formation of water bridges[9]. Stretching of the PEG polymer releases the water molecules that in the relaxed state form double hydrogen bonds[18]. Accordingly, larger stretching forces in solvent are needed compared to PEG in gas phase[9].
For poly(ethylene oxide), neutron diffraction experiments revealed that each monomer is hydrated by six solvent molecules[19]. No evidence for the presence of structured water at the polymer-water interface was found[19]. Also, the tetrahedral cavities in water are too small to accommodate the polymer; therefore, the polymer cannot be assumed to be hydrated by an unperturbed tetrahedral water lattice[19].
Depending on the following parameters: temperature, molecular weight of PEG and water content of the solution, PEG solubilized in isobutyric acid can form helices[20]. These helices coexist with coils: separate PEG molecules can form either helices or coils and/or one PEG molecules can take on a partially coiled and partially helical structure.

For PEG with 15 units, using molecular dynamics (MD) simulations[21], the hydration, conformation of PEG and the water structure near PEG were already examined. In water, PEG transforms from a collapsed coil to a helical structure, which was considered as a unique pattern for PEG solvated in water. A rather complex hydration structure was found, consisting of bridging water molecules between PEG and the bulk solvent and between two O atoms of PEG separated by two ethylene oxide units. The average number of water molecules associated per ethylene oxide unit is 2.9, in agreement with experimental studies. In our study, we will extend this work with a statistical analysis of the hydration shell using MD simulations, in combination with clustering and topological analysis of the hydrogen bond network using graph theory. The water

structure forming the solvation shell will be properly analyzed along the MD trajectories in terms of local structural parameters as the average hydrogen bonds and number of water molecules. These systems will also be characterized as a complex network, in which each water molecule can be handled as a vertex and the hydrogen bonds among them as edges[22]. For water-formamide mixtures, data from neutron-diffraction experiments and from MD simulations are in good agreement, suggesting that molecular modeling can give realistic descriptions of water-hydration [23]. Also, for PEG, validation of MD simulations by experimental data confirms that the MD approach is capable of generating reliable molecular structures and descriptions[17].
To further study the water – solute interactions and to study the effects of the polymer conformational change induced by water, we perform quantum mechanical calculations on representative structures of the MD simulation, to evaluate the electrostatic potential and the atomic charge using different electron partitioning schemes (ESP, NPA, Hirshfeld-I).

This fundamental work, aimed to give insight in the solvation properties of PEG and POM, can give leads for the practical use of PEG polymers as linkers with a fine-tuned spacer arm length in for example multivalent inhibitor design (*e.g.*, an overview can be found in Brissonnet *et al.* [24]; and references therein).

2. Methods

2.1 Molecular Dynamics Simulations

Chains of PEG and POM oligomers with a different number of monomers (2, 3, 5, 10, 15, 25, and 50 units for PEG & 3, 7, 13, and 22 units for POM) were constructed using *Gaussview*. In order to perform efficient conformational searches on the PEG and POM chains, we employed the Conformer Generation (ConfGen) tool in the Schrödinger suite. The oligomer chains were then centered in an orthorhombic box of water molecules and it was ensured that all edges of the box were at least 10 Å away from any atom of the solute. The box was filled with 3-site rigid water molecules (Transferable Intermolecular Potential with 3 points, TIP3P model). The topology files of all the systems were generated using the OPLS_2005 force field parameters[25]. This server derives parameters for the various atom types automatically from the molecule's topological structure.
The TIP3P water model is indeed a relatively simple water model, but both TIP3P and OPLS-AA were developed by Jorgensen[26,27] and his group, and they are compatible. The OPLS_2005 force field includes the TIP3P force field as one of the two default water models.

Systems were then relaxed into a local energy minimum using the Maestro's default two-stages protocol, followed by four stages of MD runs with gradually diminishing restrains. The MD simulations were carried out using the Desmond simulation package of Schrödinger. The particle mesh Ewald method was utilized to calculate the long-range electrostatic interactions[28]. Using periodic boundary conditions, all runs were performed for 150 ns, with a simulation time step of 2 fs, in the NPT ensemble with a temperature of 300 K, using the Nosé–Hoover chain coupling scheme for the temperature control. The pressure was fixed at 1 atm, using the

Martyna–Tuckerman–Klein chain coupling scheme for the pressure control[29]. Every 20 ps, a snapshot of the structure was saved to build the trajectory of the MD simulations. In order to obtain statistically independent configurations, every 70th snapshot of each trajectory (equal to a temporal spacing of 1.4 ns) was selected for further analysis, leading to 108 snapshots for each PEG and POM system. These 108 snapshots were clustered using the trajectory frame clustering tool based on the root-mean-square deviation (rmsd) matrix calculated for carbon atoms. The mid structures of the top three clusters were selected for the electrostatic potential, Hirshfeld-I, NPA, and ESP charge calculations (see further below).

2.2 Analysis of the hydrogen bonding network

For our study we used a well-accepted and frequently applied criterion to define hydrogen bonds. Two atoms, O and H, in water or PEG/POM are regarded as hydrogen bonded if the H···O distance between the two atoms is smaller than 2.5 Å and the O···O-H angle is smaller than 30°. However, some of the water molecules over the surface of PEG/POM do not directly form hydrogen (H-) bonds with PEG/POM but interact via dipole-dipole and dispersion forces (e.g. via C-H_{ether}…O_{H2O} type interactions). These water molecules were identified as having a C_{ether}···O_{water} distance smaller than 4.5 Å, a criterion used previously successfully in the studies of the hydration shell around DNA[14] and insulin[13]. All water molecules around PEG/POM that correspond to these criteria belong to the first solvation shell. The second shell of water molecules was then defined to include all water molecules that do not belong to the first solvation shell and that form a H-bond to the 1st shell water molecules using the above H-bond criteria. Using this rule, water molecules were assigned to additional shells. For further details and visual representation, please consult Figure 2 in *Rozza et al*[14].

The average hydrogen bond number, N_{HB}, was calculated by averaging the number of hydrogen bonds over the trajectory and over all molecules (Eq. 1),

$$N_{HB} = \frac{\langle \sum_{i=1}^{N} N_{HB,i} \rangle}{2N} \quad (1)$$

where N is the number of water molecules of the entire water box; the factor of 2 in the denominator is avoids double counting of the H-bonds.

.

2.3 Charge calculations

As mentioned in the previous section, three structures were chosen for each system (PEG and POM with various chain lengths) for quantum mechanical calculations to study the effect of composition, chain length and conformation on the atomic charges of the individual atoms. For

the oligomer chains with the smallest number of PEG units, charge calculations were also performed in the presence of a 6 Å shell of water molecules, to investigate the impact of water solvation on the atomic charges of the oligomers. In previous work on protein clusters, it was shown that this should be sufficient to obtain a converged picture for non-radical systems[30]. Three fundamentally different charge schemes were chosen: Natural Population Analysis (NPA), Hirshfeld-I (HI-I) and ElectroStatic Potential (ESP).

2.4 Hirshfeld-I -Charge calculations

For each structure, the first-principles electron densities as well as the local electrostatic potential are calculated. In this work, Hirshfeld-I (H-I) charges are calculated making use of a grid based approach which directly partitions the electron density[31,32]. This atoms-in-molecules approach has been shown to provide robust charges with regard to the structure of polymer conformations[33] as well as periodic materials[34] while remaining sensitive to the chemical environment, allowing for charge transfer calculations at interfaces[35].
The first-principle models are constructed by placing selected MD polymer geometries with a vacuum region of at least 15 Å in each direction in the centre of an orthorhombic cell. This reduces possible interactions between periodic copies to a negligible level and allows for the charge density to decay naturally to an almost zero value at the cell edge.

Density functional theory calculations are performed using the Projector Augmented Waves (PAW) method as implemented in Vienna Ab initio Simulation Package (VASP) code. The exchange and correlation functionals were approximated using a generalized gradient approximation as derived by Perdew, Burke and Ernzerhof (PBE)[36]. The kinetic energy cut off was set to 1000 eV with the electronic energy convergence criterion set to 10^{-8}. Atomic charges were calculated using the Hirshfeld-I atoms-in-molecules partitioning scheme, implemented in the HIVE-code, using a convergence criterion of 1.0 10^{-6} electron, and a Lebedev-Laikov grid of 2030 grid points per spherical shell[31,32,37,38].
The electrostatic potential (EP) was visualized using the VESTA program[39]. VASP allows one to store the local potential containing only the Hartree contribution (same definition for ESP as given by Gaussian) or both the Hartree and the exchange-correlation contribution. A test (see SI, Figure S1) with the 2-unit PEG shows the exchange-correlation contribution to only lead to very minor changes. The qualitative picture for both approaches thus remains the same.

2.5 NPA and ESP - Charge calculations

NPA[40,41] and ESP[42] charges are calculated from the MD structures (see previous section) using the Gaussian 16 program package[43] using the B3LYP functional and the 6-311+G(d)-basis set from the MD structures (see previous section).

3. Results & Discussion

3.1 Structure of solvated PEG and POM

From the MD simulations, it can be seen that both PEG and POM polymers behave the same way in water, whereas in reality, POM is completely insoluble in water. As we will see in the next sections, there are differences at the microscopic level. This picture is confirmed by the radial distribution functions (*cf*. Fig. S0), describing the distance between the oxygens of PEG and the hydrogen atoms of water. The curves show the existence of H-bond interactions (*cf*. peak at 2Å). For PEG, there is a clear difference in radial distribution between the middle ether oxygens and the -OH end groups/the first ether oxygen. For POM, the end-points show the same radial distribution as the middle oxygens.

Both PEG and POM have an almost free rotation around the C-C and C-O single bonds in gas phase. This is significantly altered in the condensed phase and when the chain interacts with a solvent. Helical structures are formed in the crystal phase of PEG[44] and POM[45]. As extensively described in the introduction, hydrated PEG transforms from a collapsed coil to a helical structure[9,15,16,17,18,19,20,21]. The H-bonds formed between the hydrated chains and water result in a significant competition between entropic and enthalpic contributions to the solvation energy. Versatile folding patterns of solvated oligomers are found: extended, helical or coiled conformation, or a combination thereof (*cf*., Fig. 1).

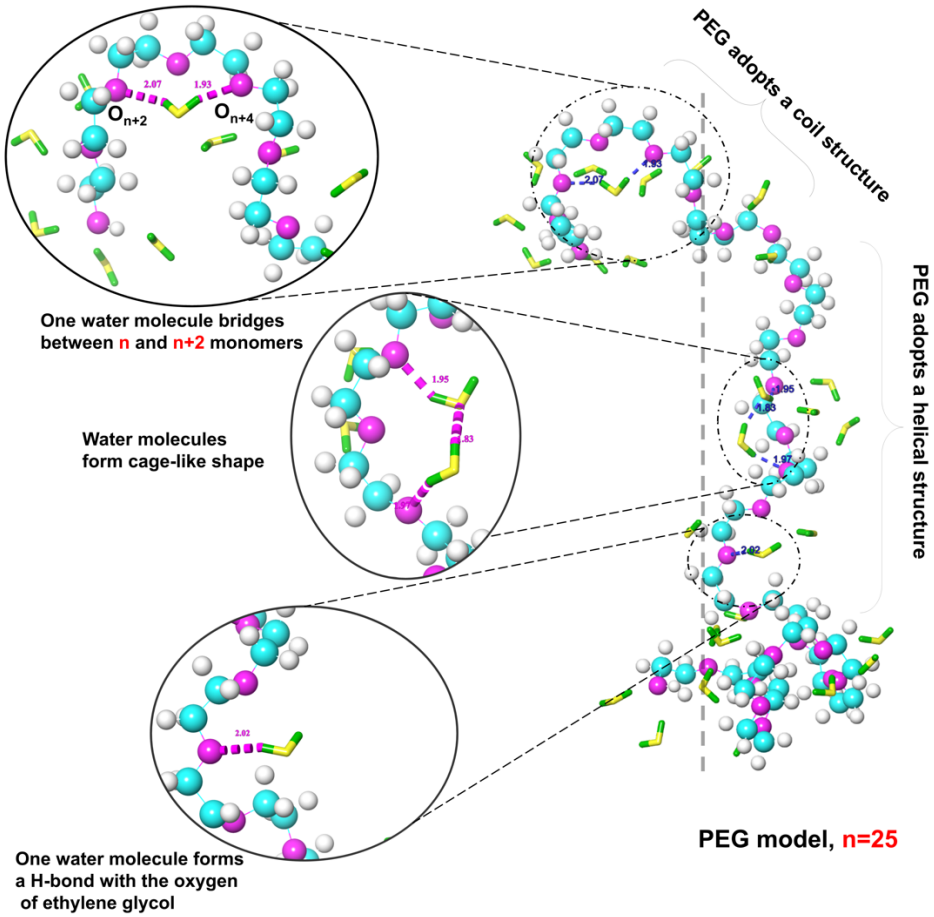

Figure 1: Possible local conformations of a PEG oligomer with 25 units (n=25), together with different ways in which water can interact with the chain, either as a single molecule interacting with a sole ether oxygen or with two ether oxygens (bridge water) or as a chain of water molecules connecting ether oxygens far away.

Several parameters can be used to characterize the shape and the size of these macromolecules. The first one is the expectation value of the square of the end-to-end distance ($\langle r^2 \rangle$). Figure S2 shows the distance (r) between the two end hydroxyl oxygen atoms (O-O) of all conformations obtained along the MD trajectory. Figure 2a shows the dependence of $\langle r^2 \rangle$ as a function of the chain length, averaged over all conformations obtained along the MD run. The degree of folding can also be assessed by a second parameter, the solvent accessible surface area (SASA) of the chain, see Figure 2b. For small chain lengths, the system behaves as a random coil (*i. e.* a statistical distribution of shapes), represented by the straight linear relation between $\langle r^2 \rangle$ or the measured SASA and the chain length. Per PEG/POM unit, we see a consecutive decrease of $\langle r^2 \rangle$ and SASA as chain length increases, which agrees with a higher degree of folding. We also see that the standard deviation on $\langle r^2 \rangle$ and SASA increases significantly as a function of chain length due to the potentially larger conformational variability of longer chains. This may be understood as a consequence of the folding of the chain and the simple model of a polymer as a self-avoiding random walk (Fig. 1 gives an overview of possible folding patterns). Already for a normal random walk, the standard deviation on the position is found to scale with the square of the chain length[46].

A third set of parameters (*cf.*, Fig. 2c,d) include the gyration radius, asphericity and acyclicity, see T1 in SI[47]. The time-evolution of the gyration radius, asphericity and acyclicity parameters along the MD trajectories for representative examples are given in Figure S3. Similar to the end-to-end hydroxyl group O-O distance (*cf.*, Fig. S2), no trends are observed, implying the structures are well equilibrated without a systematic tendency towards folding of the structures. For an ideal polymer (random coil), the gyration radius as a function of monomeric unit follows a power law behavior with an exponent of 0.5[48]. For PEG/POM, the gyration radius shows indeed power law behavior, but with a significant deviation from the ideal random coil (*cf.*, Fig. 2c). This deviation becomes more pronounced when the chains become longer, consistent with the behaviour of $\langle r^2 \rangle$ and SASA (*cf.*, Fig. 2a,b). According to the best of our knowledge, no universal law applying to the asphericity and acyclicity parameters have been established until now. From our data, it can be seen that both parameters follow a power law behavior, again except for the largest polymers.

POM has a significantly larger $\langle r^2 \rangle$ and asphericity index than PEG for chains having about the same number of heavy atoms (*e.g.*, POM-13 and PEG-10 have 26 and 30 heavy atoms, respectively). This indicates that the conformations found for PEG and POM are different, with POM having more extended conformations than PEG. The SASA of POM however, is somewhat smaller compared to PEG, in agreement with its insolubility.

In summary, all parameters considered in this section indicate the considerable folding of the longer oligomers, while smaller chains adopt a random coil. This goes along with the shift from entropic (random coil) to enthalpic (folded chain) contributions making up the majority part of the solvation energy for longer chains.

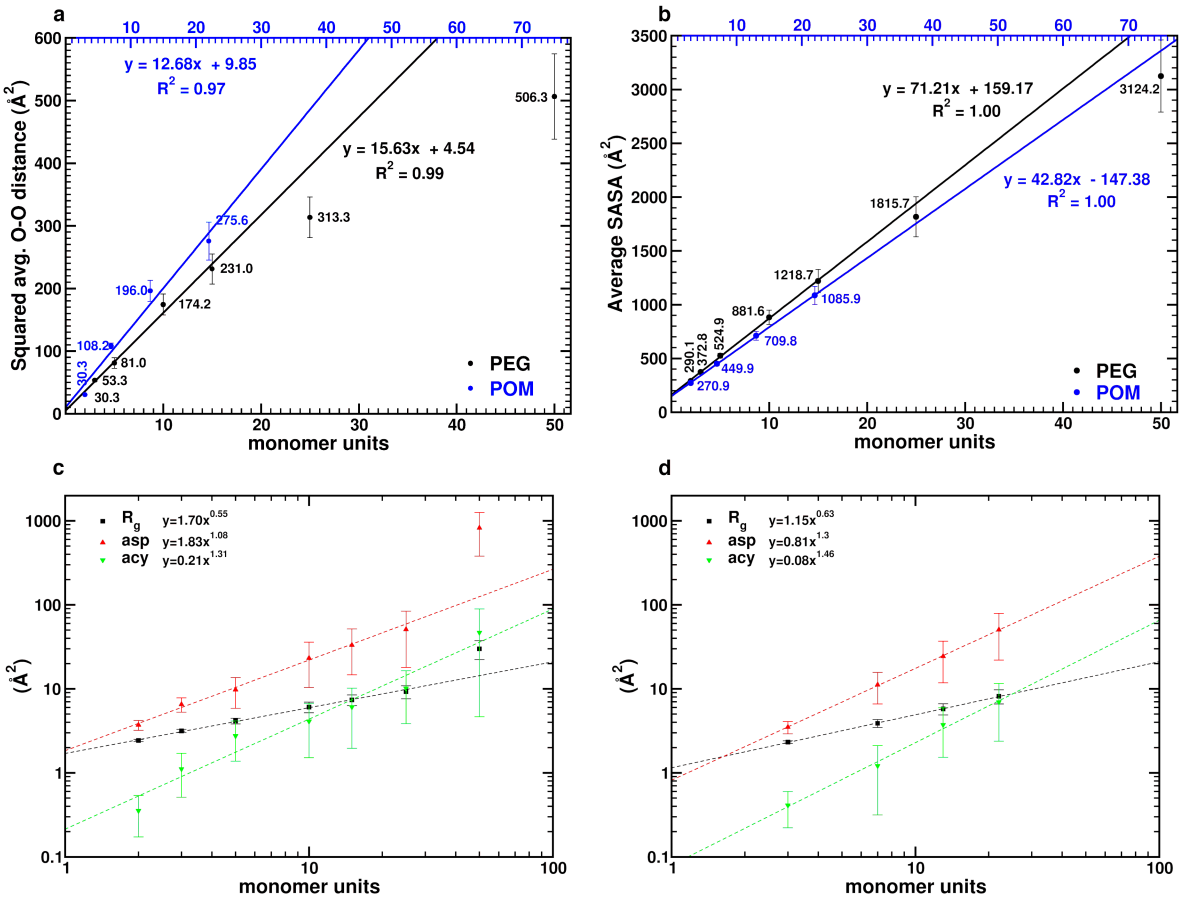

Figure 2: a) Dependence of $\langle r^2 \rangle$ as a function of the chain length, with r the distance between the end hydroxyl groups, measured between the two end hydroxyl oxygen atoms (O-O), for PEG and POM. b) Solvent Accessible Surface Area (SASA) of PEG and POM. c-d) Gyration radius, asphericity and acyclicity for PEG (c) and POM (d), shown in a log-log scale.
For a-d, all data are shown as a function of the unit number and have been averaged over all conformations obtained along the MD run. For the PEG chains, the systems up to PEG-15 are included in the fit to have a similar number of heavy atoms as the largest POM chain (POM22); PEG-22 and PEG-50 are indicated on the graph, but not included in the fit.

3.2 Hydration analysis of the solvation shells – Analysis of the water structure

3.2.1 Water molecules in the solvation shells

Water can form H-bonds with other water molecules or with the PEG/POM chain or bridging both (*cf.* Fig. 1). Water molecules of the first solvation shell are identified as PEG/POM-hydrogen-bonded, either as donor or acceptor (PHB, hydrophilic) or as PEG/POM-non-hydrogen-bonded (PnHB, hydrophobic) water molecules. PHB waters form direct hydrogen bonds to the oligomer, while PnHB waters are close ($r_{C-O} < 4.5$ Å) to the surface of the central part of the oligomer. This interaction, however, does not involve hydrogen bonds with the oligomer. The PHB and PnHB water molecules add up to the first solvation shell. The water molecules from

the bulk solvent excluding this first solvation shell, are indicated as "*all*", throughout this work. For the oligomers, the oxygen atoms are either labelled as ether O or as end group -OH.

We counted the number of water molecules in the hydration shells around the solutes, according to the criteria given in the Methodology section (*cf.*, Fig. 3). The number of water molecules per PEG unit reported in literature ranges from 1 to 6 (see ref. [21] and references herein), which appears to be lower than the values found in our study (*cf.*, Table S1). The number of PHB waters per PEG/POM unit varies between 0.5 and 1.6 (*cf.*, Table S1).

The number of water molecules in each shell is smaller for POM than for PEG (*cf.*, Fig. 3) which is consistent with its lower SASA and the insolubility in water of POM compared to PEG (see previous section and Fig. 2). For most oligomers, the number of water molecules consecutively increases when going to higher solvation shells. However, at or above a threshold chain length (10 units of PEG and 22 units of POM), more water molecules are present in the first solvation shell than in the second one (*cf.*, Fig. 3 a.I, b.I). This may be due to the volume exclusion effect, which is more pronounced for larger chains, as for these more variation in conformation are seen. For instance, for a U-shaped chain, there is not enough space in the middle of the structure to form a complete second solvation shell. Experimentally, the solubility of PEG decreases with chain length[10], which is consistent with the consecutive decrease of the number of water molecules in the solvation shells with increasing number of ethylene glycol or formaldehyde units present in the PEG/POM chains (*cf.*, Fig. 3 a.II, b.II). As such, larger chains are less hydrated per chain unit, which appears to be a consequence of geometric factors.

Although no direct data is obtained on how many water molecules interact with a particular PEG/POM unit, we anticipate an end-effect on the number of water molecules accumulated by the -OH end groups. These groups are more accessible to solvent, have three H-bond forming sites and are bound to only one bulkier group, in contrast to the ether oxygens, which have only two H-bond forming sites and are bound to two bulkier groups. Furthermore, as will be discussed in paragraph 3.3.1, the -OH end groups form more H-bond interactions than the ether oxygens (Fig. S4), giving an indirect confirmation of the accumulation of water at the edges.

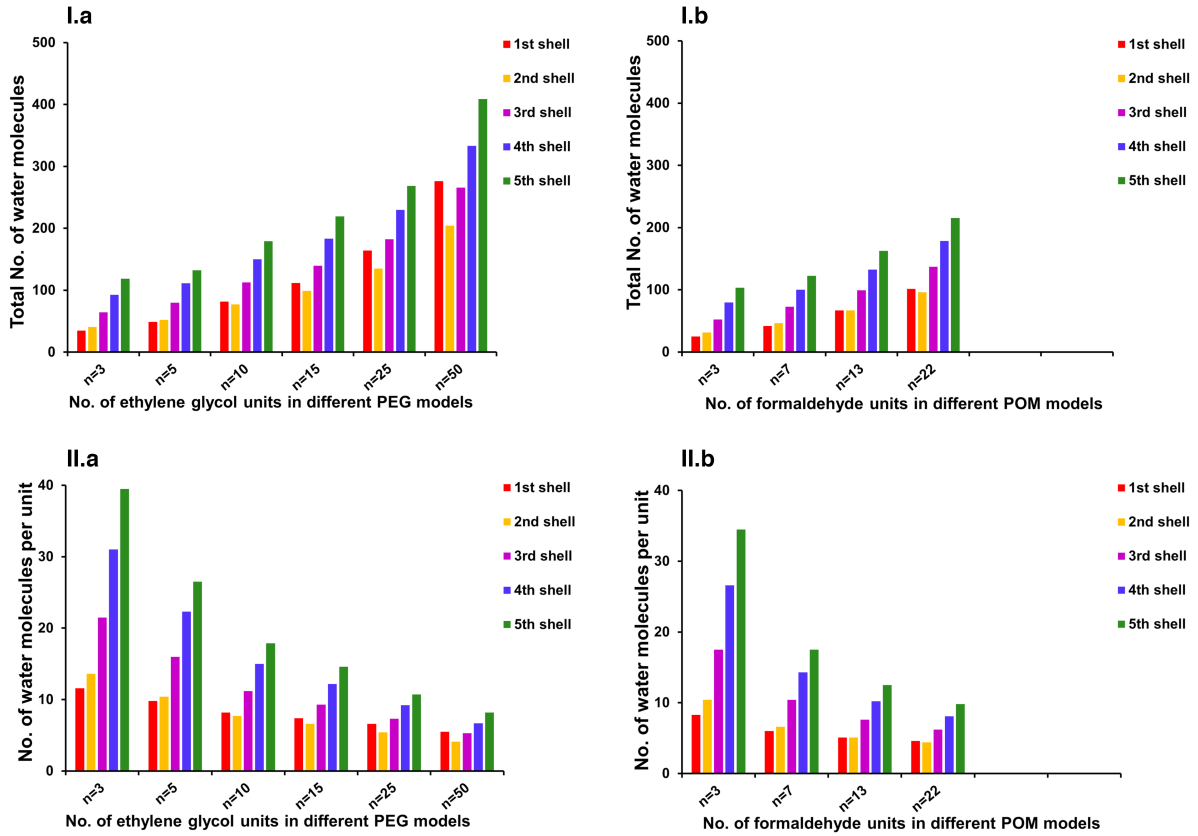

Figure 3: Number of water molecules in the various hydration shells (I) and number of water molecules per ethylene glycol or formaldehyde units (II) as a function of PEG (a) or POM (b) units, averaged over all conformations obtained along the MD trajectory. Accompanying data, see Table S1.

3.2.2 Number of H-bonds

The number of H-bonds formed per water molecule (water to water and water to solute) as a function of the chain length is presented in Fig. 4 and Table S2. For the first solvation shell around PEG, we find an average number of H-bonds formed per PHB and PnHB water molecule of 3.6 and 3.4, respectively. Similar averages of 3.7 and 3.3 per PHB and PnHB water molecule, respectively, are found for POM (*cf.*, Table S3).

Water molecules in the first solvation shell of the oligomer form fewer H-bonds than in the higher hydration shells. A possible explanation might be that a significant number of water molecules turning towards the solute surface are less available (geometrically constrained), compared to water in bulk solvent, to form interactions.

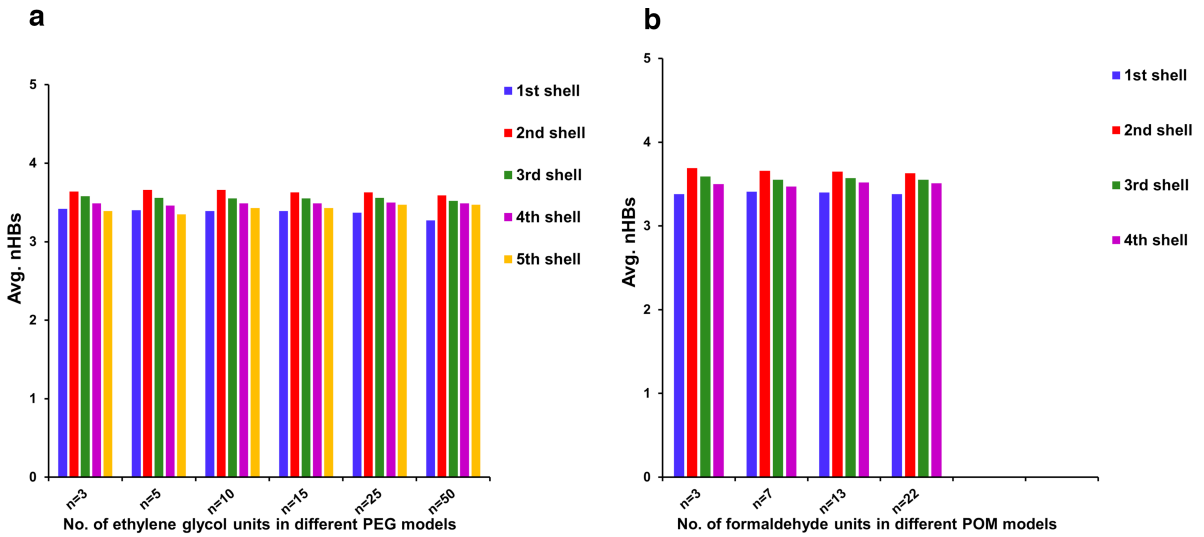

Figure 4: Number of H-bonds (nHBs) formed per water molecule (water to water and water to solute) in the various hydration shells as a function of ethylene glycol (PEG) (a) or formaldehyde (POM) (b) units, averaged over all conformations obtained from the MD simulation. Accompanying data, see Table S2.

3.3 Hydration analysis of PEG/POM chains

3.3.1 Interactions with the PEG/POM chains

The number of hydrogen bonds per ether oxygen atom and per oxygen atom of the OH-end groups is presented in Fig. S4 for representative examples. We observe that: 1) the -OH end groups form a large number of H-bonds; 2) the first ether oxygens adjacent to the end -OH, form fewer H-bonds than the following ones and 3) for the ether oxygens in the centre of the oligomer, the number of formed H-bonds randomly varies within a narrow range around the average value. It is clear from these results that a strong end-effect is seen in H-bond formation. The average over all ether oxygens (excluding the two outer O atoms at both ends to exclude end-effects, *cf.*, Fig. S4) taken within one chain, shows that the number of H-bonds tends to decrease with chain length (*cf.*, Fig. 5). This is consistent with the solubility decrease of larger chains (*cf.*, Fig. 2, 3). Furthermore, for POM fewer H-bonds per ether oxygen are found than for PEG, in agreement with its lower hydration.

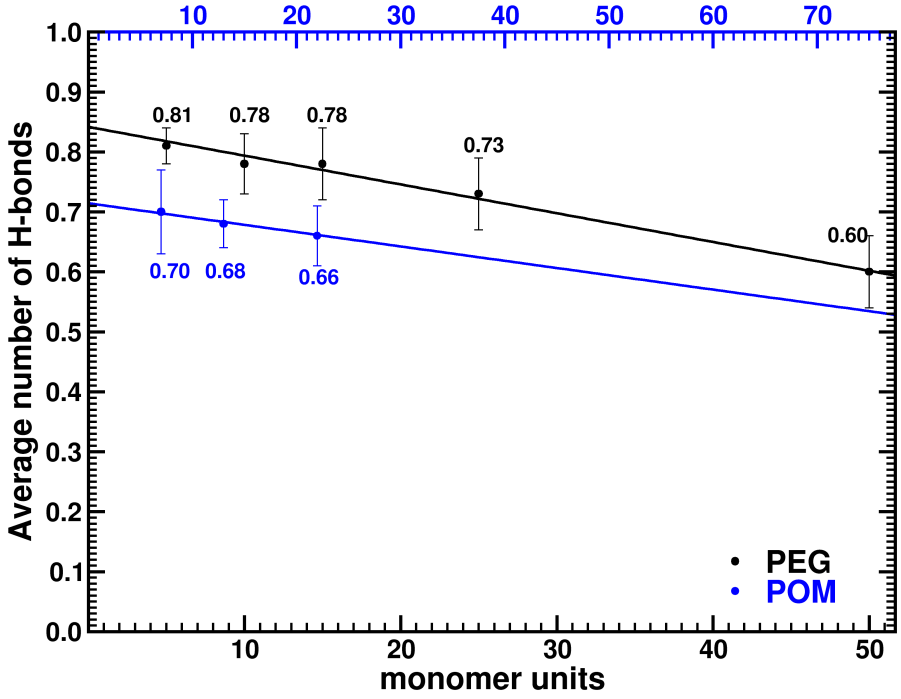

Figure 5: Average number of hydrogen bonds per ether oxygen, averaged over all ether oxygens in one chain, and over all conformations obtained from the MD simulation, excluding the -OH end groups and first adjacent ether O (*cf.*, Fig. S4), for PEG and POM oligomers of different lengths (note that PEG-3 and POM-3 are not present as these oligomers do not have middle ether oxygens, only an -OH end group and a first adjacent ether).

Solvent-solute interaction energies are attractive (negatively valued, *cf.*, Table S4). They are calculated as the sum of the Coulomb and the Lennard-Jones interaction potential, hereby following the standard approach as being used in molecular mechanics methods (*cf.* Eq(1) in Jorgensen et al.[27]). We calculated the interaction energy between PEG/POM per water molecule (thus as a mean value, independent of the number of water molecules present in a particular shell), which for the first solvation shell is a weighted sum of the interaction with both the PEG/POM H-bonded (PHB) and the PEG/POM non-H-bonded (PnHB) water molecules. The PHB as well as the PnHB interaction energies are attractive (thus negatively valued), with the oligomer—PnHB interaction energies clearly much smaller, resulting in an overall first shell solvation interaction energy per water molecule of about -1.2 to -1.6 kcal/mol, independent of chain length or oligomer type.

For the PHB water molecules forming H-bonds with the oligomer, a profoundly more negative interaction energy per water molecule is found. This interaction energy is also significantly higher, thus more negative, for PEG than for POM (*cf.*, Fig. 6), consistent with its higher degree of hydration. Here as well, we see a non-linear increase of the interaction energy with increasing numbers of oligomer units (*cf.* a non-linear curve, Fig. 6), consistent with the finding that longer chains form less H-bonds to water per ether oxygen (*cf.*, Fig. 5).

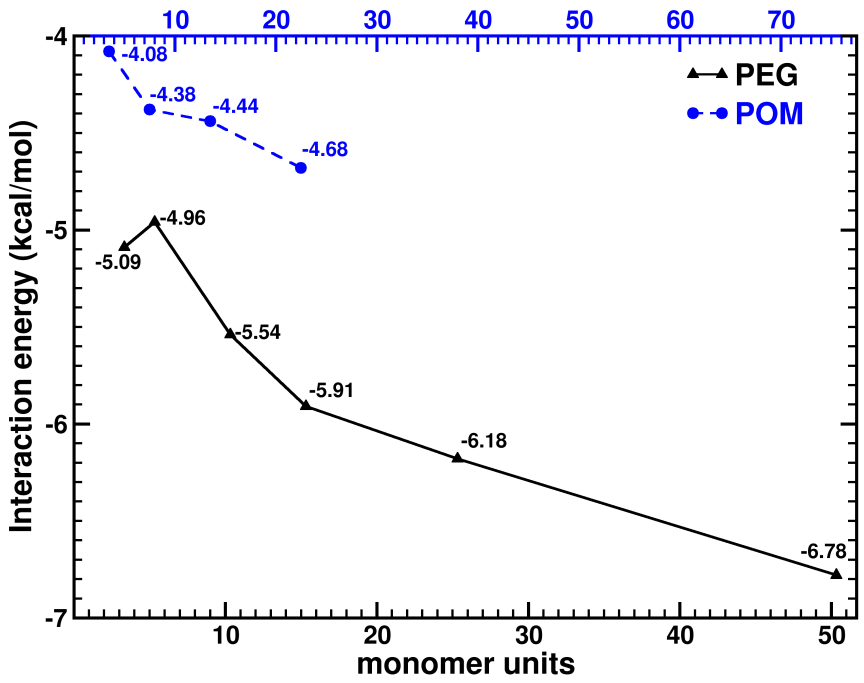

Figure 6: Interaction energy (kcal/mol) between PEG (triangles, solid line) or POM (circles, dashed line) and PHB water (interaction energy per water molecule) in function of the chain length, *cf.* Table S4.

3.3.2 Bridging waters

Water molecules forming two hydrogen bonds to PEG or POM and hereby bridging two oxygen atoms of the oligomer, are indicated as bridging water molecules (*cf.*, Fig. 1). Bridging waters have been reported experimentally from IR studies[15] and from MD simulations[21]. In agreement with this earlier work, the highest probability of finding bridging water molecules is between the n^{th} and $n+2^{nd}$ oxygen (*cf.*, Fig. 7). For POM, water molecules are bridging the n^{th} and $n+1^{st}$ oxygen. This can be easily visualized from a topological perspective. POM and PEG chains are not straight, but form a jagged-structure. If two carbon atoms separate the oxygen atoms of consecutive units, as in PEG, the oxygens of the n^{th} and $n+2^{nd}$ unit are found at the same side of the PEG chain. If only one carbon atom separates consecutive oxygens, these oxygen atoms are found at the same side of the chain, easily justifying the highest probability to bridge the n and n+1 oxygen of POM oligomers.

Furthermore, PEG and POM oligomers do not adopt a linear conformation in solvent, but are coiled. Therefore, there are also other bridges between ether oxygen atoms which are close together in space that can be formed, but with a lower probability.

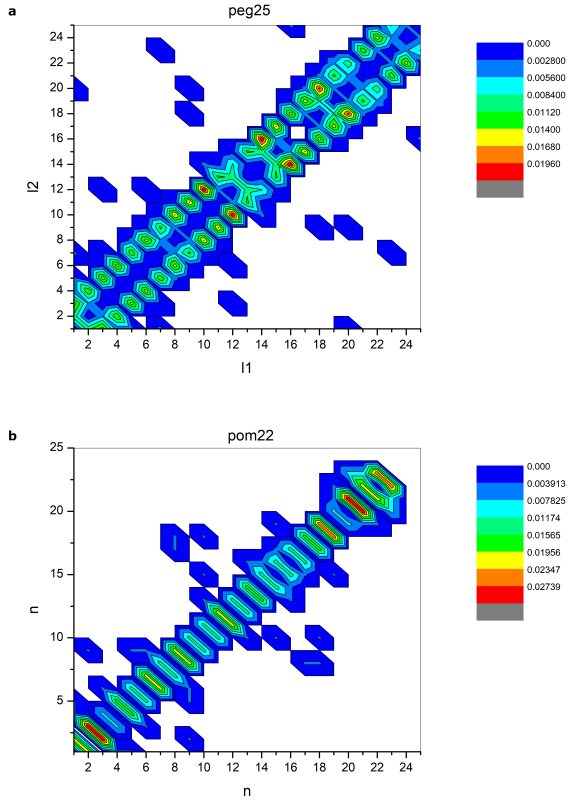

Figure 7: Probability of forming a bridge (*cf.* Fig. 1) between various ether oxygen pairs in PEG-25 (a) and POM-22 (b). Both axes are labeled with the unit number of ether oxygens and colors express the probability of finding water molecules between the respective oxygen atoms. The strong coloring, indicating the likelihood of finding a bridging water molecule, is most pronounced among ether oxygens of units n and n+2 for PEG and among ether oxygens of adjacent units for POM. Other spots show that bridge water molecules can also be found among units that are more distant from each other.

3.4 Electrostatic potential and charge

Electrostatic potentials can give further insights into the interactions of polymers with solvent molecules and can therefore be used to assess factors governing solubility. The evaluation of electrostatic potentials is, however, somewhat hampered as they are defined at every point in space. In contrast, charge schemes localize the electrons at an atomic nucleus, thus providing condensed descriptors which are more practical tools to use for direct evaluation. However, one needs to remember that atomic charges are in a sense '*fictitious*' as atomic charge is not a quantum mechanical observable. Consequently, there exists no uniquely defined partitioning scheme. In our work, we therefore use several such schemes (*c.q.* HI-I, NPA, and ESP charges), which are based on fundamentally different ways of electron partitioning, to obtain a more robust picture.

3.4.1 Geometry and chain length dependence

From the analysis presented in previous sections, we can conclude that hydration is strongly dependent on the conformation. We found that longer chains are more heterogeneous structures and more folded compared to smaller chains adopting a random coil. Longer chains are less solvated per monomeric unit as the hydration shells take up a smaller volume around the oligomer. As such, solvation depends on the geometrical shape, which is influenced by the length of the oligomer chain. This is not the case for the electrostatic potential (EP), calculated around the solute in gas phase. To judge the role of the geometry of the system on the EP around the solute, PEG-10 and POM-13 (having a similar number of heavy atoms) chains were studied, as they are long enough to show significant bending. The three conformers with highest probability during the MD simulation show a clearly different structure (*cf.*, Fig. 8a). However, there is no obvious qualitative variation in EP between the different conformations. The EP calculated on the oxygen atoms are irrespective of the conformation negatively valued, while the rest of the chain has a rather neutral EP, indicated by respectively the red and green color (*cf.*, Fig. 8a).

Consistent with the EP picture, atomic HI-I charges for gas phase oligomers present no significant variation with the conformation (*cf.*, Fig. S5). Furthermore, the atomic charges converge quickly with regard to the distance from the chain ends (*cf.*, Fig. 9), a finite size effect also observed in proteins[30]. Already for a PEG chain of 5 units, the atomic charges of the central unit present no significant deviation from the average, which roughly coincides with the values for an infinite (straight) PEG chain ($O_{HI-I} = -0.258\ e; C_{HI-I} = 0.002\ e; H_{HI-I} = 0.064\ e$). In case of an infinite POM chain the HI-I charges are $O_{HI-I} = -0.294\ e; C_{HI-I} = 0.266\ e; H_{HI-I} = 0.014\ e$.

Although some oscillations around the average values are visible, these remain within the standard deviation of the individual charges, which is of the order of 0.01-0.02 electrons. The O and H charges of the -OH end points show a significant deviation (*cf.*, Fig. 9), which can be expected from the difference in chemical nature of the group (-OH versus ether oxygen).

The different charge schemes considered here (HI-I, NPA, and ESP) agree that the atomic charges of the gas phase oligomers are independent of geometry and oligomer length (*cf.*, Fig. 9 and S6). The actual values of the charges, on the other hand, differ according to the charge scheme, which is to be expected as charges are not quantum mechanical observables.

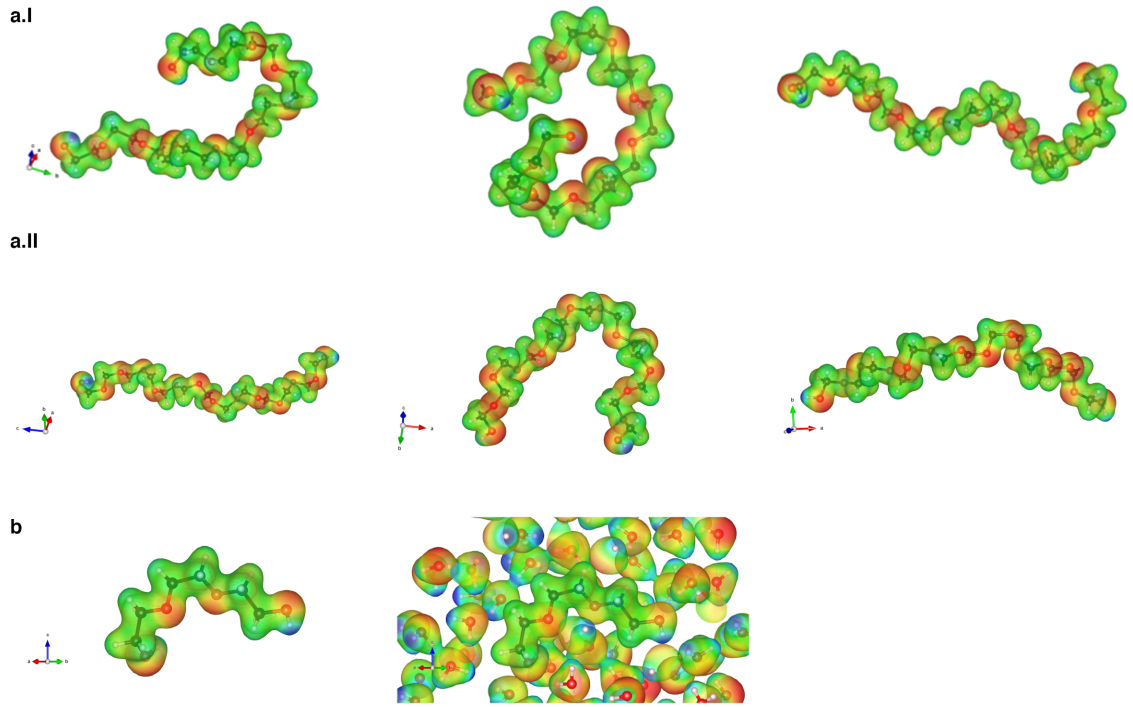

Figure 8: a) The Hartree local potential for the three configurations with highest probability of occurrence of the PEG-10 (a.I) and POM-13 (a.II) system, plotted on the iso-charge surface of 0.03 e. b) Local potential, Hartree only for the PEG-3 molecule in gas phase and in a water-cluster up to 6 Å, plotted on the iso-charge surface of 0.03 e. The color code representing the EP shows which parts have a more positive (blue) or negative (red) EP, the green color indicates a neutral EP. The EP in the presence of water becomes less negative, as indicated by the change from the red to green color upon going from vacuum to solvent.

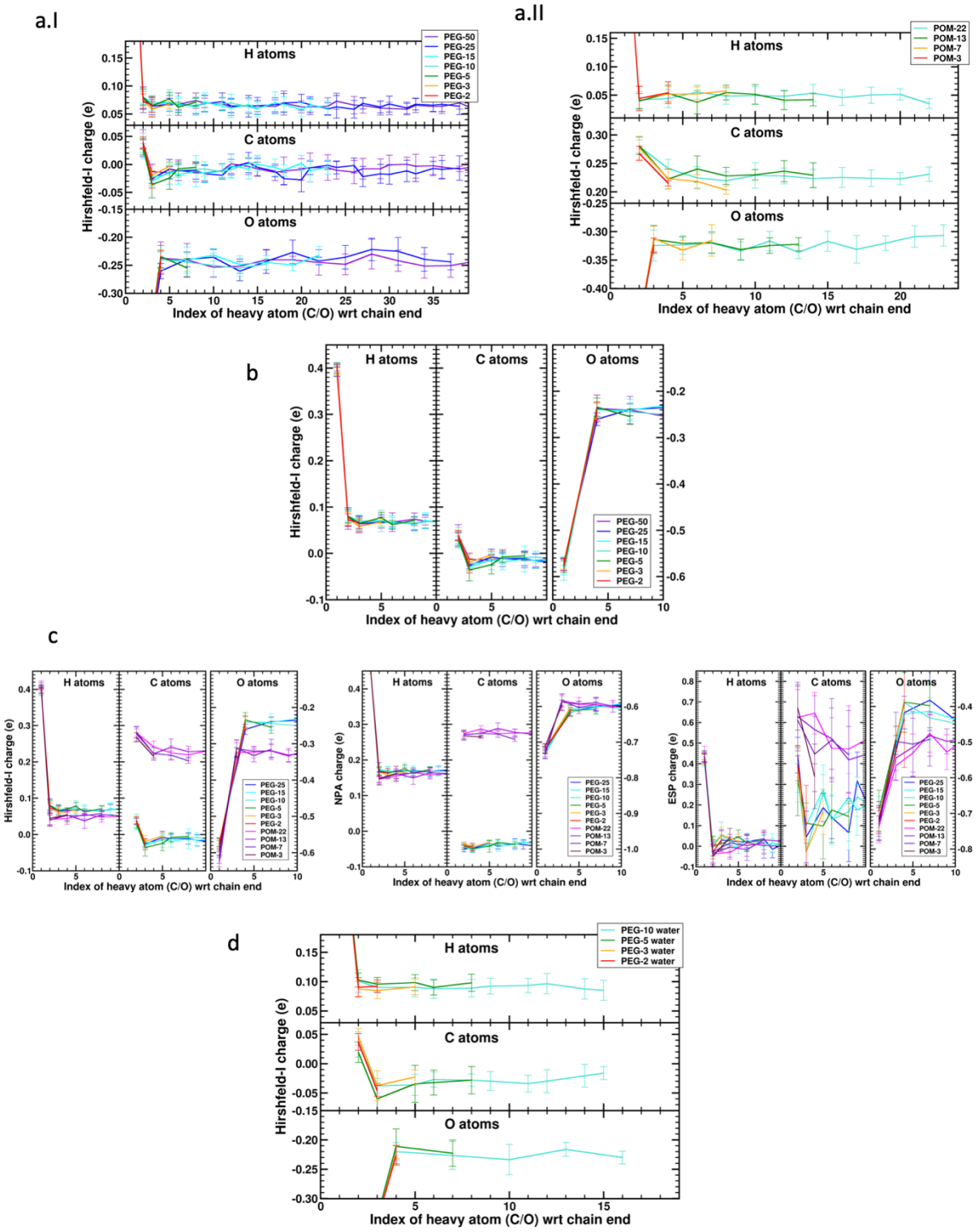

Figure 9: a) Average Hirshfeld-I charges (averaged over three conformations obtained along the MD trajectory, *cf*. Method section) for PEG (a.I) or POM (a.II) molecules of different length obtained in gas phase (see also text T2 in Supp. Inf.). The standard deviation is given as error bar. The y-ranges are identical for the H, O and C atoms, allowing for direct visual comparison of the results. A similar figure for the NPA and ESP charge distribution can be found in SI as Figure S6. b) Same as panel a), but limited to the atoms closest to the chain ends, for PEG. c) Comparison of the average charges between PEG and POM molecules of different length obtained in gas phase with the different charge schemes.

d) Average Hirshfeld-I charges (averaged over three conformations obtained along the MD trajectory, *cf*. Method section) for PEG molecules of different length obtained in a converged solvent sphere of 6Å around the PEG molecule. The standard deviation is given as error bar. The y-ranges are identical for the H, O and C atoms, allowing for direct visual comparison of the results.

3.4.2 Charge transfer to the solvation sphere

The atomic charges calculated for the solvated oligomers surrounded by a converged water shell of 6Å are presented in Fig. 9d. For oligomers ranging from PEG-2 to PEG-10, the effect of water on the EP is evaluated, as these systems are small enough to allow for the inclusion of the water shell during the DFT calculations. We clearly see that the strong negative EP (red color) seen on the oxygen atoms of the non-solvated chains is now neutralized (green color) in the presence of water (*cf.*, Fig. 8b). As such, charge is transferred to the surrounding water, leaving the solute globally more positively charged, compared to the oligomers in the gas phase. Per atom there is a small, though significant, shift of charge from the PEG/POM-molecule to the water molecules (*cf.*, Table 1), which varies with the chosen conformation.

The small charge transfer agrees with the small water-solute interaction energy found per water molecule (*cf.*, Table S4) in the range of weak/moderate H-bond interactions (Fig. 6).

The charge transfer to the solvation sphere shows overall a decreasing trend per number of ethylene glycol/formaldehyde units in a particular oligomer (*cf.*, Table 1) and is smaller for POM than for PEG, all consistent with the lower hydration of longer chains and of POM compared to PEG. As noted before, the smaller SASA for POM and non-linear decrease of the solvent accessible surface in function of the unit number, especially seen for larger chain lengths (*cf.*, Fig. 2) leads per chain unit and for POM to a lower number of 1) water molecules in the solvation shells and of 2) H-bonds formed to ether oxygens (*cf.*, Fig. 3 and 5). As a consequence, the less hydrated chains of higher unit number and of POM carry less positive charge per unit number.

Table 1: Total charge transfer from PEG/POM to water, calculated as the deviation from zero of the total charge of the solvated solute molecule, and average charge transfer per ethylene glycol or formaldehyde unit (HI-I-charges, in units of electrons) from PEG/POM to water, given per considered conformation.

Chain	Conformation 1	Conformation 2	Conformation 3	Av. charge transfer per ethylene gly-col/formalde-hyde units
PEG-2	0.15 e	0.17 e	0.24 e	0.093 e
PEG-3	0.24 e	0.26 e	0.27 e	0.086 e
PEG-5	0.43 e	0.47 e	0.54 e	0.096 e
PEG-10	0.82 e	0.84 e	0.85 e	0.084 e
POM-3	0.14 e	0.18 e	0.16 e	0.053 e

A more detailed investigation of the individual atomic charges on the PEG chains, as well as the charge of the water molecules, shows no clearly preferred charge transfer site. The charge is transferred from the solute as a whole to the surrounding water solvation shell.

3.5 Solubility of PEG and POM

The origin of the different solubilities is not well understood[49]. Numerous work show evidence that the hydrogen-bond geometry of the PEG solvating water molecules is more favorable than that of the POM solvating water molecules (for an overview, see *Ensing et al.*[11]), which would be at the basis for the solubility difference. Recent work[11] attributes however the solubility difference to inductive effects, resulting in different partial charges on the O-atoms, depending on the number of C-atoms by which they are separated. They find more negative RESP charges for the ether oxygens of PEG-3 than for POM-3, obtained by the AMBER GAFF force-field from fitting the quantum mechanically calculated electrostatic potential around PEG-3 and POM-3[11], without including the solvent molecules.

Although the OPLS force field used for the MD simulations in our work uses the same atomic charges for PEG and POM and for the different chain lengths (*cf.*, Fig. S7), we clearly see that POM in our simulations is less solvated than PEG (*cf.*, Fig. 2, 3, and 5). Further, we observe that the atomic charges of the oligomer in the gas phase are independent of conformation and chain length (*cf.*, Fig. 9a and S6), which indicates that solvation properties are not determined by the individual atomic charges. This conclusion follows from the different charge schemes independently. This strong agreement can be placed in stark contrast to the clear difference of the values of the individual atomic charges given by the different charge schemes (*cf.*, Fig. 9c). Further, there is also no agreement among the different charge schemes on the relative values of the C and O atomic charges of solvated PEG *versus* POM. Based on the HI-I and ESP schemes, we observe more negative atomic charges on the O atoms in hydrated PEG compared to POM (*cf.*, Fig. 9c), opposed to what was found by Ensing *et al.*[11]. The NPA charge scheme,

on the other hand, gives similar charges for the ether oxygens in solvated PEG and POM. This discrepancy among the different charge schemes reinforces our statement that the origin of varying solvation properties should be found outside the atomic charges

As a final remark on solubility, let us note that it is determined by numerous factors and not solely by the Coulombic interactions with the solvent molecules. The complex phenomena of dissolution are a phase equilibration process which depends on both the liquid phase of the solvent and the solid phase of the solute (*e.g.*, factors such as lattice energy, solvation free energy), as well as on their mutual interaction. Also other factors as temperature and concentration of the solute come into play. A more complete picture of the dissolution process would be obtained by the study of the thermodynamics of solid-solution equilibria. This is however beyond the scope of this contribution.

4. Conclusion

In summary, solvation appears to decrease with polymer length. Longer chains are more folded and as a consequence of these geometrical factors, water is excluded, giving rise to a smaller solvent accessible surface (SASA). Per additional chain unit, a decrease in the number of water molecules in the solvation shells as well as a lower number of H-bonds formed to the ether oxygens is found. A smaller SASA and an accordingly lower degree of hydration are also found for POM compared to PEG. Atomic charges are found to remain unchanged irrespective of the chain length and conformation, indicating that conformational effects, rather than inductive effects, are the dominant factors determining their strikingly different solubility in water. Noting that hydration induces charge transfer from the solute molecule to the solvent, this charge transfer depends on the polymer conformation and on the degree to which the chains are solvated by means of the solvent accessible surface. As such, geometrical factors will eventually determine the atomic charges of solvated chains.

Acknowledgements
The computational resources and services used in this work were partially provided by the Centre de Ressources Informatiques (CRI) and by the VSC (Flemisch Supercomputer Center), funded by the Research Foundation Flanders (FWO) and the Flemisch Government – department EWI and by the supercomputing facilities based in Debrecen, Hungary provided by NIIF of KIFÜ.
This work was performed with financial support from the Centre National de la Recherche Scientifique (CNRS), the Ministère de l'Enseignement Supérieur et de la Recherche in France and the National Agency for Research (ANR project HICARE 17-CE07-028-01).
J.O. acknowledge financial support of the "Vissza a Tudományba" grant of Budapest University of Technology and Economics, of the KU Leuven – Budapest University of Technology and Economics joint research funding (CELSA/19/017) and of project no. 2018-1.2.1-NKP-2018-00005 of the National Research, Development and Innovation Fund of Hungary. B.I. thanks the support of grant 142429 of the National Research, Development and Innovation

Office of Hungary. A.M.R. thanks the support of a Stipendium Hungaricum Fellowship, the Tempus dissertation scholarship of the Tempus Public Foundation, and of the Egyptian Government.
MJO thanks the Hungarian-American Fulbright Commission for a Fulbright Research Grant in support of her stay in Hungary and the U.S. National Science Foundation grant # CHE-1905214.

References

(1) Langer, R.; Tirrell, D. A. Designing Materials for Biology and Medicine. *Nature* **2004**, *428* (6982), 487–492. https://doi.org/10.1038/nature02388.

(2) Brandenberger, C.; Mühlfeld, C.; Ali, Z.; Lenz, A.-G.; Schmid, O.; Parak, W. J.; Gehr, P.; Rothen-Rutishauser, B. Quantitative Evaluation of Cellular Uptake and Trafficking of Plain and Polyethylene Glycol-Coated Gold Nanoparticles. *Small* **2010**, *6* (15), 1669–1678. https://doi.org/10.1002/smll.201000528.

(3) Duncan, R. Polymer Conjugates as Anticancer Nanomedicines. *Nat Rev Cancer* **2006**, *6* (9), 688–701. https://doi.org/10.1038/nrc1958.

(4) D'souza, A. A.; Shegokar, R. Polyethylene Glycol (PEG): A Versatile Polymer for Pharmaceutical Applications. *Expert Opinion on Drug Delivery* **2016**, *13* (9), 1257–1275. https://doi.org/10.1080/17425247.2016.1182485.

(5) Knop, K.; Hoogenboom, R.; Fischer, D.; Schubert, U. S. Poly(Ethylene Glycol) in Drug Delivery: Pros and Cons as Well as Potential Alternatives. *Angewandte Chemie International Edition* **2010**, *49* (36), 6288–6308. https://doi.org/10.1002/anie.200902672.

(6) Chen, W.-Y.; Hsu, M.-Y.; Tsai, C.-W.; Chang, Y.; Ruaan, R.-C.; Kao, W.-H.; Huang, E.-W.; Chung Chuan, H.-Y.-T. Kosmotrope-like Hydration Behavior of Polyethylene Glycol from Microcalorimetry and Binding Isotherm Measurements. *Langmuir* **2013**, *29* (13), 4259–4265. https://doi.org/10.1021/la304500w.

(7) Tondwal, R.; Singh, M. Effect of Increasing Alkyl Chain of 1st Tier Dendrimers on Binding and Release Activities of Methotrexate Drug: An in Vitro Study. *Journal of Molecular Liquids* **2015**, *211*, 466–475. https://doi.org/10.1016/j.molliq.2015.07.033.

(8) Devanand, K.; Selser, J. C. Polyethylene Oxide Does Not Necessarily Aggregate in Water. *Nature* **1990**, *343* (6260), 739–741. https://doi.org/10.1038/343739a0.

(9) Heymann, B.; Grubmüller, H. Elastic Properties of Poly(Ethylene-Glycol) Studied by Molecular Dynamics Stretching Simulations. *Chemical Physics Letters* **1999**, *307* (5–6), 425–432. https://doi.org/10.1016/S0009-2614(99)00531-X.

(10) *PEG Solubility | PDF | Polyethylene Glycol | Gas Chromatography*. Scribd. https://www.scribd.com/document/133761477/Peg (accessed 2022-11-19).

(11) Ensing, B.; Tiwari, A.; Tros, M.; Hunger, J.; Domingos, S. R.; Pérez, C.; Smits, G.; Bonn, M.; Bonn, D.; Woutersen, S. On the Origin of the Extremely Different Solubilities of Polyethers in Water. *Nat Commun* **2019**, *10* (1), 2893. https://doi.org/10.1038/s41467-019-10783-z.

(12) Albert, R.; Barabási, A.-L. Statistical Mechanics of Complex Networks. *Rev. Mod. Phys.* **2002**, *74* (1), 47–97. https://doi.org/10.1103/RevModPhys.74.47.

(13) Lábas, A.; Bakó, I.; Oláh, J. Hydration Sphere Structure of Proteins: A Theoretical Study. *Journal of Molecular Liquids* **2017**, *238*, 462–469. https://doi.org/10.1016/j.molliq.2017.05.038.

(14) Rozza, A. M.; Bakó, I.; Oláh, J. Theoretical Insights into Water Network of B-DNA Duplex with Watson-Crick and Hoogsteen Base Pairing Geometries. *Journal of Molecular Liquids* **2022**, *362*, 119728. https://doi.org/10.1016/j.molliq.2022.119728.

(15) Begum, R.; Matsuura, H. Conformational Properties of Short Poly(Oxyethylene) Chains in Water Studied by IR Spectroscopy. *J. Chem. Soc., Faraday Trans.* **1997**, *93* (21), 3839–3848. https://doi.org/10.1039/A703436I.

(16) Oesterhelt, F.; Rief, M.; Gaub, H. E. Single Molecule Force Spectroscopy by AFM Indicates Helical Structure of Poly(Ethylene-Glycol) in Water. *New J. Phys.* **1999**, *1* (1), 6. https://doi.org/10.1088/1367-2630/1/1/006.
(17) Oelmeier, S. A.; Dismer, F.; Hubbuch, J. Molecular Dynamics Simulations on Aqueous Two-Phase Systems - Single PEG-Molecules in Solution. *BMC Biophysics* **2012**, *5* (1). https://doi.org/10.1186/2046-1682-5-14.
(18) Liese, S.; Gensler, M.; Krysiak, S.; Schwarzl, R.; Achazi, A.; Paulus, B.; Hugel, T.; Rabe, J. P.; Netz, R. R. Hydration Effects Turn a Highly Stretched Polymer from an Entropic into an Energetic Spring. *ACS Nano* **2017**, *11* (1), 702–712. https://doi.org/10.1021/acsnano.6b07071.
(19) Bieze, T. W. N.; Barnes, A. C.; Huige, C. J. M.; Enderby, J. E.; Leyte, J. C. Distribution of Water around Poly(Ethylene Oxide): A Neutron Diffraction Study. *J. Phys. Chem.* **1994**, *98* (26), 6568–6576. https://doi.org/10.1021/j100077a024.
(20) Alessi, M. L.; Norman, A. I.; Knowlton, S. E.; Ho, D. L.; Greer, S. C. Helical and Coil Conformations of Poly(Ethylene Glycol) in Isobutyric Acid and Water. *Macromolecules* **2005**, *38* (22), 9333–9340. https://doi.org/10.1021/ma051339e.
(21) Tasaki, K. Poly(Oxyethylene)−Water Interactions: A Molecular Dynamics Study. *J. Am. Chem. Soc.* **1996**, *118* (35), 8459–8469. https://doi.org/10.1021/ja951005c.
(22) Bakó, I.; Bencsura, Á.; Hermannson, K.; Bálint, S.; Grósz, T.; Chihaia, V.; Oláh, J. Hydrogen Bond Network Topology in Liquid Water and Methanol: A Graph Theory Approach. *Phys. Chem. Chem. Phys.* **2013**, *15* (36), 15163. https://doi.org/10.1039/c3cp52271g.
(23) Bakó, I.; Oláh, J.; Lábas, A.; Bálint, S.; Pusztai, L.; Bellissent Funel, M. C. Water-Formamide Mixtures: Topology of the Hydrogen-Bonded Network. *Journal of Molecular Liquids* **2017**, *228*, 25–31. https://doi.org/10.1016/j.molliq.2016.10.052.
(24) Brissonnet, Y.; Assailly, C.; Saumonneau, A.; Bouckaert, J.; Maillasson, M.; Petitot, C.; Roubinet, B.; Didak, B.; Landemarre, L.; Bridot, C.; Blossey, R.; Deniaud, D.; Yan, X.; Bernard, J.; Tellier, C.; Grandjean, C.; Daligault, F.; Gouin, S. G. Multivalent Thiosialosides and Their Synergistic Interaction with Pathogenic Sialidases. *Chemistry – A European Journal* **2019**, *25* (9), 2358–2365. https://doi.org/10.1002/chem.201805790.
(25) Banks, J. L.; Beard, H. S.; Cao, Y.; Cho, A. E.; Damm, W.; Farid, R.; Felts, A. K.; Halgren, T. A.; Mainz, D. T.; Maple, J. R.; Murphy, R.; Philipp, D. M.; Repasky, M. P.; Zhang, L. Y.; Berne, B. J.; Friesner, R. A.; Gallicchio, E.; Levy, R. M. Integrated Modeling Program, Applied Chemical Theory (IMPACT). *Journal of Computational Chemistry* **2005**, *26* (16), 1752–1780. https://doi.org/10.1002/jcc.20292.
(26) Jorgensen, W. L.; Chandrasekhar, J.; Madura, J. D.; Impey, R. W.; Klein, M. L. Comparison of Simple Potential Functions for Simulating Liquid Water. *The Journal of Chemical Physics* **1983**, *79* (2), 926–935. https://doi.org/10.1063/1.445869.
(27) Jorgensen, W. L.; Maxwell, D. S.; Tirado-Rives, J. Development and Testing of the OPLS All-Atom Force Field on Conformational Energetics and Properties of Organic Liquids. *J. Am. Chem. Soc.* **1996**, *118* (45), 11225–11236. https://doi.org/10.1021/ja9621760.
(28) Toukmaji, A. Y.; Board, J. A. Ewald Summation Techniques in Perspective: A Survey. *Computer Physics Communications* **1996**, *95* (2–3), 73–92. https://doi.org/10.1016/0010-4655(96)00016-1.
(29) Mao, H.; Hemley, R. J.; Mao, A. L. Recent Design of Ultrahigh-pressure Diamond Cell. *AIP Conference Proceedings* **2008**, *309* (1), 1613. https://doi.org/10.1063/1.46394.

(30) Vanpoucke, D. E. P.; Oláh, J.; De Proft, F.; Van Speybroeck, V.; Roos, G. On the Convergence of Atomic Charges with the Size of the Enzymatic Environment. *J. Chem. Inf. Model.* **2015**, *55*, 564–571. https://doi.org/10.1021/ci5006417.
(31) Vanpoucke, D. E. P.; Bultinck, P.; Van Driesche, I. Extending Hirshfeld-I to Bulk and Periodic Materials. *J. Comput. Chem.* **2013**, *34*, 405–417. https://doi.org/10.1002/jcc.23088.
(32) Vanpoucke, D. E. P.; Van Driesche, I.; Bultinck, P. Reply to 'Comment on "Extending Hirshfeld-I to Bulk and Periodic Materials." *J. Comput. Chem.* **2013**, *34*, 422–427. https://doi.org/10.1002/jcc.23193.
(33) Stouten, J.; Vanpoucke, D. E. P.; Van Assche, G.; Bernaerts, K. V. UV-Curable Biobased Polyacrylates Based on a Multifunctional Monomer Derived from Furfural. *Macromolecules* **2020**, *53* (4), 1388–1404. https://doi.org/10.1021/acs.macromol.9b02659.
(34) Wolffis, J. J.; Vanpoucke, D. E. P.; Sharma, A.; Lawler, K. V.; Forster, P. M. Predicting Partial Atomic Charges in Siliceous Zeolites. *Microporous and Mesoporous Materials* **2019**, *277*, 184–196. https://doi.org/10.1016/j.micromeso.2018.10.028.
(35) Damle, V.; Wu, K.; De Luca, O.; Ortí-Casañ, N.; Norouzi, N.; Morita, A.; de Vries, J.; Kaper, H.; Zuhorn, I. S.; Eisel, U.; Vanpoucke, D. E. P.; Rudolf, P.; Schirhagl, R. Influence of Diamond Crystal Orientation on the Interaction with Biological Matter. *Carbon* **2020**, *162*, 1–12. https://doi.org/10.1016/j.carbon.2020.01.115.
(36) Perdew, J. P.; Burke, K.; Ernzerhof, M. Generalized Gradient Approximation Made Simple. *Phys. Rev. Lett.* **1996**, *77*, 3865–3868. https://doi.org/10.1103/PhysRevLett.77.3865.
(37) Lebedev, V. I.; Laikov, D. N. Quadrature Formula for the Sphere of 131th Algebraic Order of Accuracy. *Dokl. Akad. Nauk* **1999**, *366*, 741–745.
(38) Bultinck, P.; Van Alsenoy, C.; Ayers, P. W.; Carbó-Dorca, R. Critical Analysis and Extension of the Hirshfeld Atoms in Molecules. *J. Chem. Phys.* **2007**, *126* (14), 144111. https://doi.org/10.1063/1.2715563.
(39) Momma, K.; Izumi, F. *VESTA* : A Three-Dimensional Visualization System for Electronic and Structural Analysis. *J Appl Crystallogr* **2008**, *41* (3), 653–658. https://doi.org/10.1107/S0021889808012016.
(40) Reed, A. E.; Weinhold, F. Natural Localized Molecular Orbitals. *J. Chem. Phys.* **1985**, *83* (4), 1736–1740. https://doi.org/10.1063/1.449360.
(41) Reed, A. E.; Weinstock, R. B.; Weinhold, F. Natural Population Analysis. *J. Chem. Phys.* **1985**, *83*, 735–746. https://doi.org/10.1063/1.449486.
(42) Breneman, C. M.; Wiberg, K. B. Determining Atom-Centered Monopoles from Molecular Electrostatic Potentials. The Need for High Sampling Density in Formamide Conformational Analysis. *Journal of Computational Chemistry* **1990**, *11* (3), 361–373. https://doi.org/10.1002/jcc.540110311.
(43) Frisch, M. J.; Trucks, G. W.; Schlegel, H. B.; Scuseria, G. E.; Robb, M. A.; Cheeseman, J. R.; Scalmani, G.; Barone, V.; Petersson, G. A.; Nakatsuji, H.; Li, X.; Caricato, M.; Marenich, A. V.; Bloino, J.; Janesko, B. G.; Gomperts, R.; Mennucci, B.; Hratchian, H. P.; Ortiz, J. V.; Izmaylov, A. F.; Sonnenberg, J. L.; Williams; Ding, F.; Lipparini, F.; Egidi, F.; Goings, J.; Peng, B.; Petrone, A.; Henderson, T.; Ranasinghe, D.; Zakrzewski, V. G.; Gao, J.; Rega, N.; Zheng, G.; Liang, W.; Hada, M.; Ehara, M.; Toyota, K.; Fukuda, R.; Hasegawa, J.; Ishida, M.; Nakajima, T.; Honda, Y.; Kitao, O.; Nakai, H.; Vreven, T.; Throssell, K.; Montgomery Jr., J. A.; Peralta, J. E.; Ogliaro, F.; Bearpark, M. J.; Heyd, J. J.;

Brothers, E. N.; Kudin, K. N.; Staroverov, V. N.; Keith, T. A.; Kobayashi, R.; Normand, J.; Raghavachari, K.; Rendell, A. P.; Burant, J. C.; Iyengar, S. S.; Tomasi, J.; Cossi, M.; Millam, J. M.; Klene, M.; Adamo, C.; Cammi, R.; Ochterski, J. W.; Martin, R. L.; Morokuma, K.; Farkas, O.; Foresman, J. B.; Fox, D. J. Gaussian 16 Rev. A.03, 2016.

(44) Takahashi, Y.; Tadokoro, H. Structural Studies of Polyethers, (-(CH2)m-O-)n. X. Crystal Structure of Poly(Ethylene Oxide). *Macromolecules* **1973**, *6* (5), 672–675. https://doi.org/10.1021/ma60035a005.

(45) Tashiro, K.; Kamae, T.; Asanaga, H.; Oikawa, T. Structural Analysis of Polyoxymethylene Whisker Single Crystal by the Electron Diffraction Method. *Macromolecules* **2004**, *37* (3), 826–830. https://doi.org/10.1021/ma030490q.

(46) *Introduction to Statistical Physics von João Paulo Casquilho | ISBN 978-1-107-05378-6 | Fachbuch online kaufen - Lehmanns.de*. https://www.lehmanns.de/shop/naturwissenschaften/30085925-9781107053786-introduction-to-statistical-physics (accessed 2022-11-19).

(47) Theodorou, D. N.; Suter, U. W. Shape of Unperturbed Linear Polymers: Polypropylene. *Macromolecules* **1985**, *18* (6), 1206–1214. https://doi.org/10.1021/ma00148a028.

(48) Dobrynin, A. V.; Rubinstein, M. Theory of Polyelectrolytes in Solutions and at Surfaces. *Progress in Polymer Science* **2005**, *30* (11), 1049–1118. https://doi.org/10.1016/j.progpolymsci.2005.07.006.

(49) *Intermolecular and Surface Forces*; Elsevier, 2011. https://doi.org/10.1016/C2009-0-21560-1.